REPORTS OF PRACTICAL ONCOLOGY AND RADIOTHERAPY 24 (2019) 399–408

Available online at www.sciencedirect.com

ScienceDirect

journal homepage: http://www.elsevier.com/locate/rpor

Original research article

On the use of AAA and AcurosXB algorithms for three different stereotactic ablative body radiotherapy (SABR) techniques: Volumetric modulated arc therapy (VMAT), intensity modulated radiation therapy (IMRT) and 3D conformal radiotherapy (3D-CRT)

Abdulrahman Tajaldeen[a,b,c], *Prabhakar Ramachandran*[a,b,*], *Salem Alghamdi*[c], *Moshi Geso*[a]

[a] *School of Health & Biomedical Sciences, RMIT University, Victoria, Australia*
[b] *Peter MacCallum cancer centre, Victoria, Australia*
[c] *Faculty of Applied Medical Science, Radiological Sciences Department, Imam Abdulrahman bin Faisal University, Saudi Arabia*

ARTICLE INFO

Article history:
Received 15 July 2016
Received in revised form
15 August 2018
Accepted 7 February 2019
Available online 23 March 2019

Keywords:
Volumetric modulated arc therapy (VMAT)
Intensity modulated radiation therapy (IMRT)
3D conformal radiotherapy (3D-CRT)
Stereotactic ablative body radiotherapy (SABR)

ABSTRACT

Aim: The purpose of this study was to investigate the dosimetric characteristics of three stereotactic ablative body radiotherapy (SABR) techniques using the anisotropic analytical algorithm (AAA) and Acuros XB algorithm. The SABR techniques include coplanar volumetric modulated arc therapy (C-VMAT), non-coplanar intensity modulated radiation therapy (NC-IMRT) and non-coplanar three-dimensional conformal radiotherapy (NC-3D CRT).
Background: SABR is a special type of radiotherapy where a high dose of radiation is delivered over a short time. The treatment outcome and accuracy of the dose delivered to cancer patients highly depend on the dose calculation algorithm and treatment technique.
Materials and methods: Twelve lung cancer patients underwent 4D CT scanning, and three different treatment plans were generated: C-VMAT, NC-IMRT, NC-3D CRT. Dose calculation was performed using the AAA and Acuros XB algorithm. The dosimetric indices, such as conformity index (CI), homogeneity index, dose fall-off index, doses received by organs at risk and planning target volume, were used to compare the plans. The accuracy of AAA and Acuros XB (AXB) algorithms for the lung was validated against measured dose on a CIRS thorax phantom.
Results: The CIs for C-VMAT, NC-IMRT and NC-3D CRT were 1.21, 1.28 and 1.38 for the AAA, respectively, and 1.17, 1.26 and 1.36 for the Acuros XB algorithm, respectively. The overall

* *Corresponding author at*: Princess Alexandra Hospital, Woolloongabba, QLD 4102, RMIT University, Victoria, Australia.
E-mail address: prabhakar_smr@hotmail.com (P. Ramachandran).
https://doi.org/10.1016/j.rpor.2019.02.008

dose computed by AcurosXB algorithm was close to the measured dose when compared to the AAA algorithm. The overall dose computed by the AcurosXB algorithm was close to the measured dose when compared to the AAA algorithm.

Conclusion: This study showed that the treatment planning results obtained using the Acuros XB algorithm was better than those using the AAA algorithm in SABR lung radiotherapy.

1. Background

Stereotactic ablative body radiotherapy (SABR) is a specialised form of radiotherapy treatment which delivers a high radiation dose using a small number of fractions, generally equal to or fewer than five fractions.[1,2] SABR is becoming more popular for the treatment of patients with lung cancer.[3,4] In recent years, the incidence rates of lung cancers have increased worldwide.[5] For early-stage inoperable non-small cell lung cancer,[6,7] SABR involves the use of different treatments, which are delivered via various methods, such as three-dimensional conformal radiation therapy (3D-CRT),[8] intensity modulated radiation therapy (IMRT) [9] and volumetric modulated arc therapy (VMAT).[10] VMAT is an arc-based IMRT technique, which has the ability to modulate the beam intensity as it rotates around the patient.[11] In VMAT, fewer monitor units (MU) are generated, and it offers faster delivery times and superior dose distributions as compared to conventional 3D-CRT/IMRT treatment plans.[12]

SABR is typically applied to small tumours and, hence, employs small radiation fields. However, air cavities present in such small fields can cause electronic disequilibrium at tissue-air interfaces.[13–15] Consequently, when treating heterogeneous media, dose calculation algorithms have to be able to account for tissue heterogeneities and provide an accurate computation of electron transport close to the tissue-air interface. One of the most common algorithms used in the Eclipse™ treatment planning system (Varian Medical Systems, Palo Alto,CA) is the anisotropic analytical algorithm (AAA). The AAA, a convolution/superposition-based algorithm is an improved pencil beam algorithm, which uses multiple pencil beam dose kernels to determine the dose contribution from different radiation sources of a clinical beam.[16,17] The limitations and the performance of the AAA have been well documented elsewhere.[16,18,19] The AAA offers significant improvements in dose accuracy compared to single pencil beam models. These include modelling of the penumbra, low-dose regions and field profiles (symmetric and asymmetric) in both open and wedged fields.[16] However, the AAA also has weaknesses, as demonstrated by the findings of Dunn et al., who showed that implementing the AAA in regions distal from lung tissue interfaces resulted in systematic under-dosing, with an average discrepancy of $2.9 \pm 1.2\%$.[19]

Recently, Varian has introduced the Acuros XB dose calculation algorithm for external beam treatment planning. This algorithm utilises the linear Boltzmann transport equation (LBTE) to solve and describe the macroscopic behaviour of radiation particles, such as electrons and neutrons, numerically as they travel and interact with matter.[20] For matter with a known volume in a given domain, the LBTE can be used to accurately describe the dose inside this domain.[20,21]

Several studies have shown that the Acuros XB algorithm is comparable to the Monte Carlo method and that both these methods are convergent and provide solutions closer to the measurements.[20–22] These studies also showed that the Acuros XB algorithm was more applicable to inhomogeneous media (i.e. it performed better) than the AAA algorithm. Moreover, the Acuros XB was reported to provide a faster calculation time compared to the Monte Carlo method and a relatively shorter computation time compared to the AAA for treatment plans involving a large number of fields.[23]

According to our review of the literature, although there are several studies comparing AAA and Acuros XB dose calculation algorithms, only limited studies involve multiple treatment techniques. In this study, we aim to: (1) investigate the dosimetric variation among three different SABR techniques: coplanar volumetric modulated arc therapy (C-VMAT), non-coplanar intensity modulated radiation therapy (NC-IMRT) and non-coplanar three-dimensional (3D) conformal radiotherapy (NC-3D CRT) and (2) conduct a phantom study to validate the accuracy of Acuros XB and AAA dose calculation algorithms in a thorax phantom.

2. Materials and methods

Twelve lung cancer patients treated by SABR were selected for this study. Of these patients, seven had lesions in the right lung, and five had lesions in the left lung. The prescription dose was 26 Gy in one fraction, and the plans were normalised to deliver the prescription dose to 99% of the PTV. The patients were positioned in a Bodyfix® blue bag, with their arms above their heads. All the patients underwent 4D-CT scanning using the bellows system on a Philips Brilliance™ CT scanner. The pulmonary wave trace was edited to ensure the tags were located at the peak of each wave before reconstructing the scan. Maximum intensity projection (MIP) images and average intensity projection (AIP) images were generated from multiple respiratory phases acquired during 4D imaging for contouring and dose calculation, respectively. The CT DICOM datasets were transferred to the Eclipse treatment planning system for contouring and treatment planning. In Eclipse, both the AIP and MIP images were used for treatment planning. The internal target volume (ITV) was delineated on the MIP images. A planning target volume (PTV) was generated from the ITV by applying a 5-mm margin to account for patient setup error. OARs, such as the lungs, heart, oesophagus, spinal cord and liver, were delineated on the AIP images. The AIP images were also used for dose calculation. As part of

the contouring process, internal skin or rind skin of OAR was defined as a 5-mm rim of tissues inside the body contour.

For each SABR patient, three different types of plans were created: (1) C-VMAT, (2) NC-IMRT and (3) NC-3D CRT. In the NC-3D CRT plans, a minimum of nine beams were used, and utmost care was taken to ensure the field size was no less than 3 cm × 3 cm, as defined by the X and Y jaws. Of these nine beams, two were non-coplanar, with a couch angle of 90 and 270° to reduce the dose to the chest wall; six were placed ipsilateral, and one (the ninth beam) entered from the contralateral side to compensate for the dose gradient. The beam orientations were optimised according to the location of the PTV. As a starting point, the multileaf collimator (MLC) was conformed to zero margins on the PTV using the outbound method of leaf positioning, and the MLC leaf positions were individually adjusted to provide adequate target coverage.

Two plans were generated using the AAA and Acuros XB algorithms. NC-IMRT plans were generated by maintaining the same beam angle arrangements defined for 3D-CRT for both the AAA and Acuros XB algorithms. Similarly, C-VMAT plans were generated for both the AAA and Acuros XB algorithm using the same dose constraints as those employed for NC-IMRT. The C-VMAT plans were composed of two arcs. The first arc was defined with the gantry start angle at 181° and the stop angle at 0° clockwise for right-sided lesions. For left-sided lesions, the start angle was 0°, and the stop angle was 179°. The second arc was defined with the gantry start angle at 0° and the stop angle at 181° counterclockwise for right-sided lesions. For left-sided lesions, the start angle was 179°, and the stop angle was 0°. The collimator angles were 30° and 330° for arc 1 and arc 2, respectively. The maximum gantry speed was 4.8°/s, and the maximum dose rate was 600 MU/min. All the plans were planned using 6 MV X-rays. In the case of Acuros XB, the dose was prescribed to medium. A cumulative dose volume histogram was used to quantify the dosimetric variations among the three SABR techniques.

The tumour dosimetry was evaluated using the conformity index (CI), dose fall-off index and homogeneity index (HI). The CI indirectly indicates the prescription dose spillage outside the target volume and, ideally, it should be close to 1. The dose conformity to the target volume was assessed using the CI as described below[24]:

$$\mathrm{CI} = \frac{\text{Percentage volume of the body receiving the presciption dose}}{\text{Volume percentage of the PTV receiving the prescription dose}} \quad (1)$$

The dose fall-off index and HI, as recommended by the American Association of Physicists in Medicine (AAPM) Task Group 101 protocol,[25] were used to assess the dose gradient around the tumour and dose inhomogeneity inside the tumour volume.

The dose fall-off index was defined as follows:

$$\text{Dose fall-off} = \frac{\text{Volume of50\% presciption isodose}}{\text{Planning target volume (PTV)}} \quad (2)$$

The HI was defined as follows:

$$\mathrm{HI} = \frac{\text{Highest dose received by5\% of PTV (D5)}}{\text{Lowest dose received by95\% of PTV (D95)}} \quad (3)$$

The dose fall-off index explains the dose spillage around the PTV and, therefore, a lower dose fall-off index indicates less dose spillage outside the PTV. When the HI is close to 1, there is better dose homogeneity inside the PTV and, hence, a high index represents higher dose heterogeneity of the PTV. The maximum dose (Dmax) and the dose received by 2 cm^3 of OAR were recorded for the heart, oesophagus and spinal cord. Also, the percentage volume of the right, left and the whole lung that received 5 Gy (V5) and 20 Gy (V20) were recorded for all studied cases. Right lung V5 and V20 were calculated for right lung tumours, and Left lung V5 and V20 were calculated for left lung tumours.

To validate the dose calculation algorithms used in this study, a CIRS Thorax phantom (Model 002LFC)[26] with a customised insert to accommodate a Diamond detector was scanned in a Philips Brilliance CT scanner. The insert was designed in Perspex precisely machined to house a PTW 60019^{TM} waterproof detector with a sensitive volume of 0.004 mm^3. To simulate a centrally located tumour volume, the Diamond detector was placed at the centre of the left lung (Fig. 1). Three plans that include AAA, Acuros XB Dw (Dose to Water) and Acuros XB Dmed (Dose to Medium) were generated in Eclipse with nine fields spaced uniformly in steps of 40° degree gantry angle commencing at 0°. All 6 MV beams were set to 100 MU with a fixed field size of 3 × 3 cm^2 to simulate the minimum field size used in this study. The Diamond detector was calibrated against a secondary standard calibrated ionisation chamber and also characterised for reproducibility, angular response, energy, field size and dose rate dependence. The dose was measured on a Clinac 21iX linear accelerator, and the measured dose was compared to the calculated dose obtained from the treatment planning system for all three treatment plans. The measurements were conducted on an IGRT couch to avoid any dose influence with couch rails.

The statistical analysis was performed by Graph Pad PRISM 6 software, v. 6.03. A one-way ANOVA, with repeated measures utilising multiple comparison was used to investigate the statistical significances ($p < 0.05$) and mean differences between the three treatment techniques (C-VMAT, NC-IMRT and NC-3D CRT).

3. Results

The dose distribution of the three treatment techniques (C-VMAT, NC-IMRT and NC-3D CRT) for a typical case is illustrated in Fig. 2. The two upper rows demonstrate the beam orientations of each technique, calculated by the Acuros XB algorithm and AAA, and the lower two rows illustrate the isodose lines for the PTV of the three techniques obtained using the AAA and Acuros XB. Figs. 3 and 4 depict the dose volume histograms of the right and left lungs, heart and PTV obtained using the three different treatment techniques (NC-3D CRT, NC-IMRT and C-VMAT) and the AAA and Acuros XB algorithms, respectively.

The CIs for C-VMAT, NC-IMRT and NC-3D CRT were 1.21, 1.28 and 1.38, respectively, for the AAA, and 1.17, 1.26 and 1.36, respectively, for the Acuros XB algorithm (Table 1). An optimum treatment plan should have a low index, ideally close to one. The one-way ANOVA revealed a significant difference in

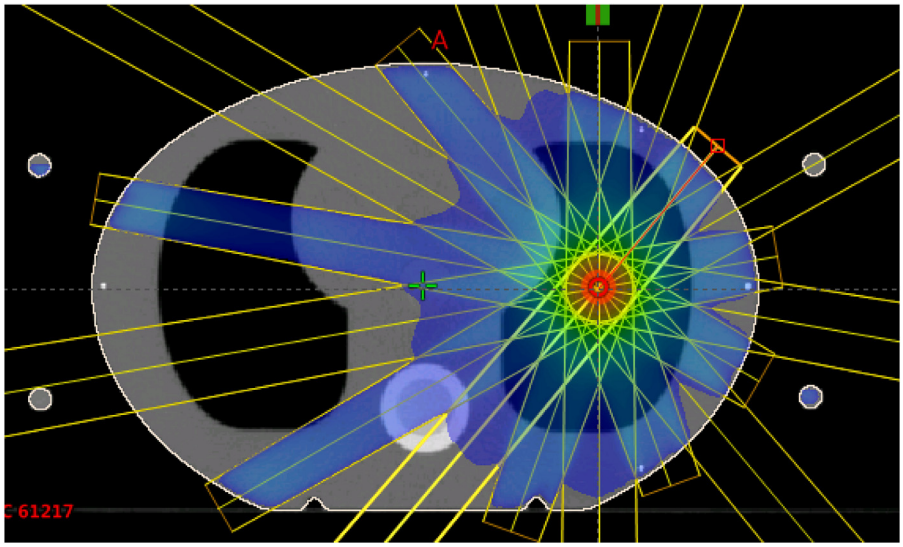

Fig. 1 – Beam arrangements on a CIRS lung phantom.

the CI between C-VMAT and NC-3D CRT plans using the AAA, whereas the Acuros XB algorithm showed statistically significant differences between all the three plans. There were also statistically significant differences in all three plans according to the HI, using both the AAA and Acuros XB algorithm. The dose spillage outside the target volume was determined by the calculation of the dose fall-off index (Eq. (2)). The mean dose fall-off index for C-VMAT, NC-IMRT, NC-3D CRT using the AAA was 5.25 ± 0.4, 5.36 ± 0.51, and 6.06 ± 0.44, respectively, and the Acuros XB was 5.15 ± 0.39, 5.18 ± 0.34 and 5.66 ± 0.63, respectively. Table 1 illustrates the dose received by 2% of the target volume (D2), 5% of the target volume (D5), 95% of the target volume (D95), 98% of the target volume (D98) and the target mean dose for all three plans planned with the AAA and Acuros XB algorithms. For the AAA, the statistical analysis using Graph Pad PRISM 6 software showed no significant differences in D95 and D98 among the three treatment techniques. The CI for C-VMAT was significantly lower than the CI for the NC-3D CRT. The Acuros XB algorithm revealed significant variation between treatment techniques for a majority of the above parameters, except for D95 and D98 PTV. These findings showed that C-VMAT resulted in a better CI and lower dose spillage, with more homogeneity inside the PTV as compared to the NC-IMRT and NC-3D CRT techniques using both the AAA and Acuros XB algorithm. On the other hand, the NC-3D CRT treatment technique resulted in a higher CI, HI and dose fall-off, representative of poor dosimetry as compared to the other two treatment plans using both the AAA and Acuros XB algorithm.

Table 2 shows the V5 and V20 for the right, left and whole lungs calculated by the AAA and Acuros XB algorithm for the C-VMAT, NC-IMRT and NC-3DCRT plans. It clearly shows that statistically significant ($p < 0.05$) amount of the right lung volume receives the 5 Gy (V5) and 20 Gy (V20) doses with C-VMAT compared to the NC-IMRT and NC-3DCRT methods, using both the AAA and Acuros XB algorithm. The V5 and V20 for the left and whole lungs with C-VMAT plan are relatively higher than the NC-IMRT and NC-3D CRT. The liver, ribs and chest wall volumes that received the 20 Gy and 30 Gy doses were almost zero in all cases. Table 3 shows the maximum dose delivered to the heart, oesophagus and spinal cord with the C-VMAT, NC-IMRT and NC-3DCRT methods using both the AAA and Acuros XB algorithm. These results clearly indicated that the C-VMAT treatment method planned using both the AAA and Acuros XB algorithm delivered a statistically significant dose to the oesophagus and spinal cord as compared to the NC-IMRT and NC-3D CRT treatment plans. Table 4 illustrates the mean dose delivered to internal skin via the C-VMAT, NC-IMRT and NC-3DCRT techniques. The mean internal skin dose was relatively lower using the NC-IMRT and NC-3D CRT methods as compared to the C-VMAT technique by 34% and 28%, respectively, for the AAA algorithm, and by 32% and 29%, respectively, for the Acuros XB algorithm.

Table 5 shows the discrepancies between AAA, Acuros XB calculation algorithms and the measured dose. The overall dose difference between the total measured dose and AAA, AXB_Dw (Acuros XB; dose prescribed to water), AXB_Dmed (Acuros XB; dose prescribed to medium) were 2.3%, 1.3% and 0.7%, respectively. For a majority of the fields, the dose measured with the Diamond detector shows relatively less discrepancy when the Acuros XB is used for planning as compared to the AAA algorithm.

4. Discussion

This study compared three different SABR treatment techniques for lung cancer: C-VMAT, NC-IMRT and NC-3D CRT, utilising two algorithms, AAA and Acuros XB, integrated into the Eclipse treatment planning system. Fig. 1 shows the comparison of the isodose lines for the three SABR treatment techniques. It indicates relatively better dose conformity to the PTV using the C-VMAT and NC-IMRT plans compared with the NC-3D CRT plan. The prescription dose of 26 Gy

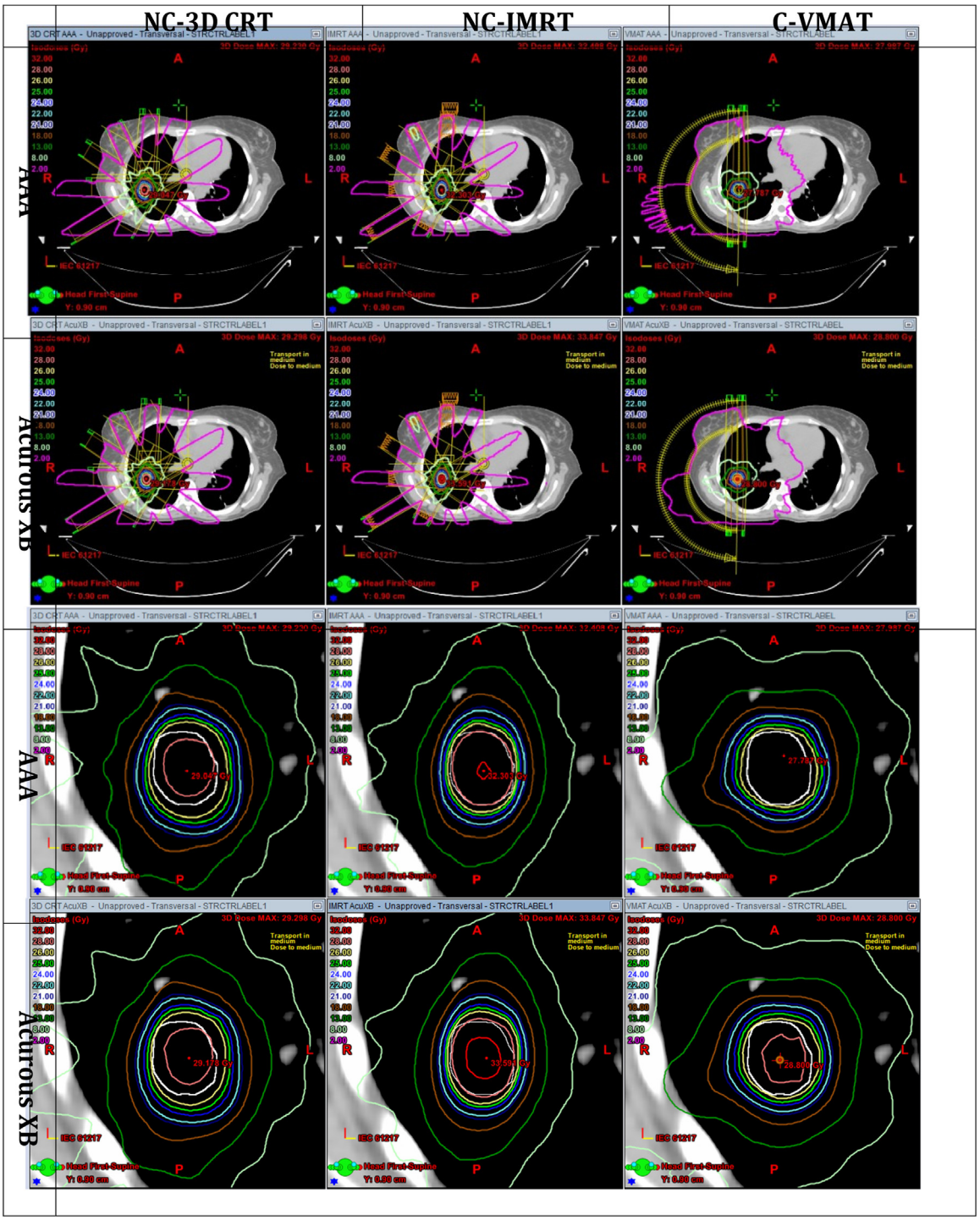

Fig. 2 – The dose distribution for the three treatment techniques C-VMAT, NC-IMRT and NC-3D CRT on the transversal plan. The isodose distributions indicate better dose conformity to the PTV (zoom in of white coloured contour) for the C-VMAT and NC-IMRT compared with the NC-3D CRT; the prescription dose of 26 Gy (zoom in of yellow coloured isodose line) is more conformal around the PTV with the C-VMAT technique for both algorithms. Minimum field size restricted to 3 cm × 3 cm.

(yellow contour) was more conformal around the PTV in the C-VMAT technique using both algorithms. The one-way ANOVA revealed statistically significant differences between the AAA and Acuros XB algorithm for the HI, dose fall-off index, D2 and D5. Better homogeneity, lower D2 and D5 and less dose fall-off were observed using the C-VMAT method. The results also revealed that the CI obtained using the Acuros XB algorithm was better than that achieved using the AAA with all three SABR techniques. This finding may be explained by the Acuros XB being a better dose calculation model for very low-density models of the dose at the lung-tissue interface.[27] Our planning study results also indicated that C-VMAT resulted in the best

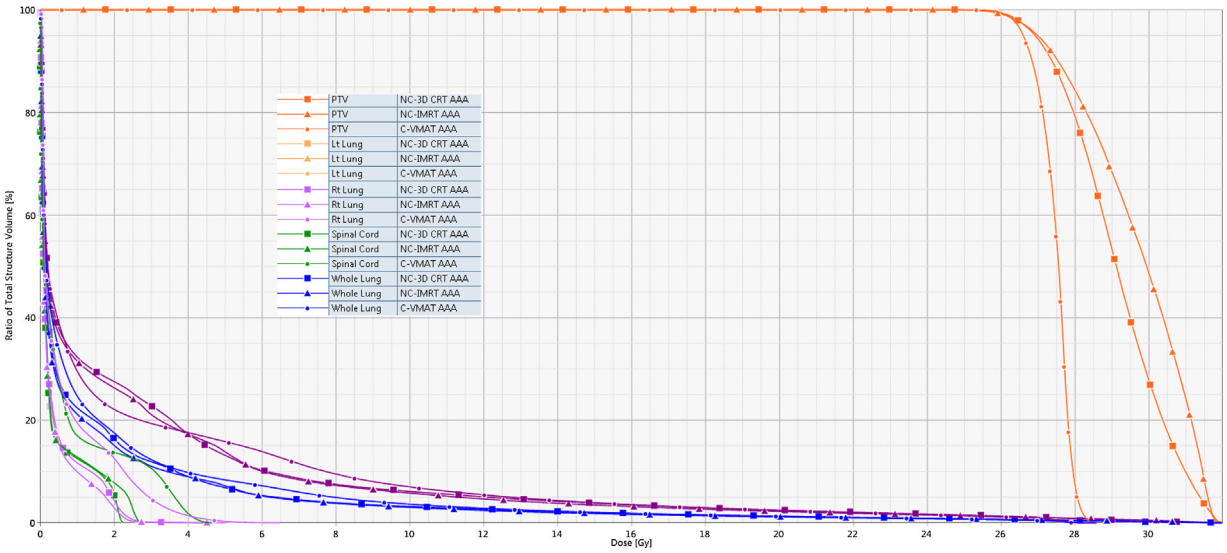

Fig. 3 – DVH of OARs for left lung and right lung, whole lung, spinal cord and PTV of the three different techniques calculated by AAA algorithms.

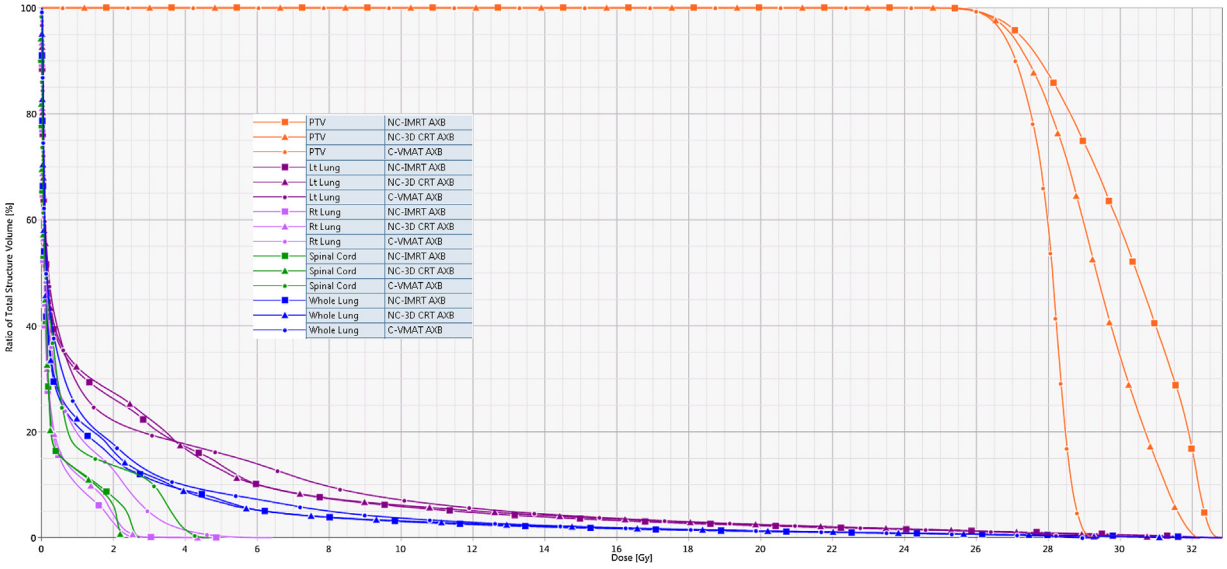

Fig. 4 – DVH of OARs for left lung and right lung, whole lung, spinal cord and PTV of the three different techniques calculated by Acuros XB algorithms.

dose conformity around the PTV and tightest dose distribution, with low spillage, followed by NC-IMRT. The highest D2 PTV (near maximum dose) value recorded for NC-IMRT (AAA) and NC-IMRT (Acuros XB) was 32 Gy and 33 Gy, respectively. The D98 value (near minimum dose) was almost the same for all the treatment techniques (~26 Gy) calculated by the AAA and Acuros XB algorithms. With all three treatment methods, the dose received by 95% of the PTV was almost similar using the AAA and Acuros XB algorithms, and the dose received by 5% of the PTV was between 28 Gy and 33 Gy.

With C-VMAT, the percentage volume that received 5 Gy (V5) and 20 Gy (V20) doses to the right, left and whole lungs was high as compared to the other treatment techniques using both dose calculation algorithms. The aforementioned is a drawback of C-VMAT, but this is offset by a reduced treatment time, better dose conformity and reduced intra-fraction motion. The dosimetric values V20 and V30 for the liver, ribs and chest wall were close to zero in all cases. Hence, these parameters were not considered in the data analysis in this study. There was no significant difference in the max dose or dose delivered to the heart (2 cm^3) with the three SABR techniques and two algorithms. With respect to the dose received by the OAR, the C-VMAT and NC-IMRT delivered the maximum dose to the surrounding healthy tissues. Holt et al. compared

Table 1 – Dmean, D2, D5, D95, D98 and plan evaluation parameters for the three different techniques C-VMAT, NC-IMRT and NC-3D CRT calculated by AAA and Acuros XB algorithms.

	C-VMAT Mean ± Std. dev.	NC-IMRT Mean ± Std. dev.	NC-3D CRT Mean ± Std. dev.
AAA algorithms calculation			
Conforming Index	1.21 ± 0.08[+]	1.28 ± 0.12	1.38 ± 0.22
Homogeneity Index	1.07 ± 0.05[*,+]	1.15 ± 0.05	1.17 ± 0.04
Dose fall off	5.25 ± 0.4[*,+]	5.36 ± 0.51	6.06 ± 0.44
D2 PTV (Gy)	28.99 ± 2.07[*,+]	32.43 ± 1.43	32.09 ± 1.26
D5 PTV (Gy)	28.6 ± 1.97[*,+]	32.26 ± 1.39	31.93 ± 1.26
D95 PTV (Gy)	27.06 ± 0.88	27.23 ± 0.28	27.31 ± 0.57
D98 PTV (Gy)	26.48 ± 0.15	26.56 ± 0.18	26.68 ± 0.21
D mean (Gy)	27.91 ± 1.16[*]	29.88 ± 1.27	27.18 ± 8.32
Acurous XB algorithms calculation			
Conforming Index	1.17 ± 0.07[*,+]	1.26 ± 0.13	1.36 ± 0.15
Homogeneity Index	1.05 ± 0.04[*,+]	1.09 ± 0.03	1.1 ± 0.04
Dose fall off	5.15 ± 0.39[*,+]	5.18 ± 0.34	5.66 ± 0.63
D2 PTV (Gy)	30.01 ± 1.84[*,+]	33.49 ± 1.85	32.36 ± 1.37
D5 PTV (Gy)	29.82 ± 1.75[*,+]	33.29 ± 1.81	32.12 ± 1.34
D 95 PTV (Gy)	27.06 ± 0.64	27.64 ± 0.42	27.39 ± 0.29
D 98 PTV (Gy)	26.56 ± 0.6	26.81 ± 0.27	26.85 ± 0.21
D mean (Gy)	28.65 ± 1.13[*,+]	30.98 ± 1.18	29.9 ± 0.77

[*] Statistical significance of C-VMAT based on one-way ANOVA multiple comparisons with repeated measure (p-value < 0.05) compared to the corresponding NC-IMRT plans.
[+] Statistical significance of C-VMAT based on one-way ANOVA multiple comparisons with repeated measure (p-value < 0.05) compared to the corresponding NC-3D CRT plans.

Table 2 – The volume percentage of the right, left and whole lungs that received 5 and 20 Gy for the three techniques computed by the AAA and Acuros XB algorithms.

	C-VMAT Mean ± Std. dev.	NC-IMRT Mean ± Std. dev.	NC-3D CRT Mean ± Std. dev.
AAA algorithms calculation			
Right lung V5 (%)	13.44 ± 1.06[+]	12.3 ± 1.04	11.87 ± 1.52
Right lung V20 (%)	5.17 ± 0.61[*,+]	3.11 ± 1.68	3.06 ± 1.44
Left lung V5 (%)	11.48 ± 1.17	11.4 ± 1.79	11.14 ± 1.22
Left lung V20 (%)	2.68 ± 1.47[*]	2.52 ± 1.41	2.44 ± 1.11
Normal lung V5 (%)	5.95 ± 1.68	5.69 ± 1.33	5.55 ± 1.87
Normal lung V20 (%)	1.86 ± 0.99	1.48 ± 0.74	1.44 ± 0.86
Acurous XB			
Right lung V5 (%)	13.41 ± 1.11[+]	12.2 ± 1.04	11.78 ± 1.49
Right lung V20 (%)	5.04 ± 0.61[*,+]	3.06 ± 1.66	3.01 ± 1.43
Left lung V5 (%)	11.36 ± 1.16	11.23 ± 1.8	11.06 ± 1.21
Left lung V20 (%)	2.58 ± 1.47	2.49 ± 1.42	2.44 ± 0.99
Normal lung V5 (%)	5.91 ± 1.69	5.61 ± 1.36	5.48 ± 1.9
Normal lung V20 (%)	1.78 ± 0.97	1.44 ± 0.74	1.4 ± 0.86

[*] Statistical significance of C-VMAT based on one-way ANOVA multiple comparisons with repeated measure (p-value < 0.05) compared to the corresponding NC-IMRT plans.
[+] Statistical significance of C-VMAT based on one-way ANOVA multiple comparisons with repeated measure (p-value < 0.05) compared to the corresponding NC-3D CRT plans.

coplanar VMAT and NC-IMRT and reported a small increase in the mean dose (V20) delivered to a healthy lung using C-VMAT.[28] Moreover, they demonstrated that the maximal dose was delivered to the spinal cord using C-VMAT rather than NC-IMRT in all cases, although the dose was below the acceptable limit of 18 Gy of physical dose. The results from the present study are in agreement with those of Holt et al. for healthy lung tissue (V20). The results of the current study also revealed an increase in the dose delivered to the spinal cord (within tolerance limits) using the C-VMAT technique as compared to the NC-IMRT and NC-3D CRT methods.

Table 4 illustrates the dosimetric impact of the C-VMAT technique on the internal body. As shown in the table, the mean doses received by the internal volume of the body minus 5 mm were low using the non-coplanar techniques compared to the coplanar VMAT method. However, in all cases, it was well below the clinically acceptable limit of 24 Gy of physical dose. The maximal dose to the oesophagus was also tolerable, with a clinically acceptable limit of 18 Gy of physical dose.[28] As evidenced by the tumour dosimetry; the C-VMAT technique resulted in better CIs, HIs and dose fall-off indices. However, this technique was also associated with relatively high doses

Table 3 – Dose to heart, oesophagus and spinal cord with C-VMAT, NC-IMRT and NC-3D CRT.

	C-VMAT Mean ± Std. dev.	NC-IMRT Mean ± Std. dev.	NC-3D CRT Mean ± Std. dev.
AAA algorithms calculation			
Heart (max dose) (Gy)	6.71 ± 5.46	5.94 ± 4.5	5.67 ± 4.37
Heart (2 cm^3) (Gy)	6.79 ± 6.45	5.75 ± 4.93	5.18 ± 4.17
Oesophagus (max dose) (Gy)	5.08 ± 5.63*,+	4.23 ± 5.92	3.44 ± 4.63
Oesophagus (2 cm^3) (Gy)	3.85 ± 4.52*,+	2.63 ± 3.68	2.49 ± 3.02
Spinal canal (max dose) (Gy)	7.02 ± 3.02*,+	4.33 ± 2.57	4.31 ± 2.53
Spinal canal (2 cm^3) (Gy)	5.48 ± 2.52*,+	3 ± 1.9	2.99 ± 1.92
Acurous XB algorithms calculation			
Heart (max dose) (Gy)	6.69 ± 5.39	5.78 ± 4.47	5.37 ± 4.26
Heart (2 cm^3) (Gy)	5.83 ± 5.31	5.68 ± 4.91	5.07 ± 4.12
Oesophagus (max dose) (Gy)	4.84 ± 5.18	3.7 ± 4.45	3.41 ± 4.6
Oesophagus (2 cm^3) (Gy)	3.56 ± 3.88*,+	2.61 ± 3.66	2.45 ± 3.01
Spinal canal (max dose) (Gy)	6.96 ± 3.03*,+	4.3 ± 2.58	4.22 ± 2.48
Spinal canal (2 cm^3) (Gy)	5.34 ± 2.46*,+	3 ± 1.93	2.9 ± 1.86

* Statistical significance of C-VMAT based on one-way ANOVA multiple comparisons with repeated measure (p-value < 0.05) compared to the corresponding NC-IMRT plans.
+ Statistical significance of C-VMAT based on one-way ANOVA multiple comparisons with repeated measure (p-value < 0.05) compared to the corresponding NC-3D CRT plans.

Table 4 – Mean dose to internal skin for three different techniques: C-VMAT, NC-IMRT and NC-3D CRT.

	C-VMAT Mean ± Std. dev.	NC-IMRT Mean ± Std. dev.	NC-3D CRT Mean ± Std. dev.
AAA algorithms calculation			
Internal skin (Gy)	0.81 ± 0.49*	0.53 ± 0.17	0.58 ± 0.21
Acuros XB algorithms calculation			
Internal skin (Gy)	0.82 ± 0.5*	0.55 ± 0.19	0.58 ± 0.21

* Statistical significance of C-VMAT based on one-way ANOVA multiple comparisons with repeated measure (p-value < 0.05) compared to the corresponding NC-IMRT plans.
+ Statistical significance of C-VMAT based on one-way ANOVA multiple comparisons with repeated measure (p-value < 0.05) compared to the corresponding NC-3D CRT plans.

Table 5 – CIRS phantom study showing the dose differences between AAA, Acuros XB (dose prescribed to water) and Acuros XB (dose prescribed to medium) and measurement.

Fields	Measured dose, MD (cGy)	Percent dose difference		
		MD vs AAA (%)	MD vs AXB_DW (%)	MD vs AXB_Dmed (%)
Anterior	80.0	2.4	2.0	1.5
OBL 40	82.8	4.1	3.7	3.1
OBL 80	81.1	4.8	4.1	3.5
OBL 120	74.6	−2.0	−2.2	−2.8
OBL 160	77.5	0.5	−0.4	−1.0
OBL 200	72.4	0.6	−0.4	−1.1
OBL 240	44.4	1.6	−0.2	−1.1
OBL 280	47.4	5.6	1.8	1.6
OBL 320	58.3	4.3	2.5	2.0
Total dose	**618.5**	**2.3**	**1.3**	**0.7**

to the surrounding normal tissues. According to Cai et al., if the delivery of a low dose to a large amount of healthy tissue is not of clinical concern, C-VMAT can aid short-term delivery, making this technique more convenient and having less of a biological effect in the presence of decreased intra-fraction motion due to prolonged fraction delivery.[29]

Both the treatment planning system and algorithms used in dose calculations can influence dosimetric results. In the present study, the Acuros XB algorithm was better than the AAA as regards the investigation of the three treatment techniques. As shown by the results of the indices used to compare the treatment plans (CI, HI and dose fall-off), the Acuros XB demonstrated lower values for all these three parameters. Liu et al. investigated dosimetric parameters using the AAA and Acuros XB algorithm in 77 treatment plans of SABR patients.[30] They used two prescription doses: 48 Gy in four fractions and 60 Gy in 10 fractions. They reported lower CIs using the Acuros XB algorithm than using the AAA. A study by Rana et al. recorded similar results when using the Acuros XB algorithm in lung cancer cases treated with SABR.[15]

The results of the present study are in agreement with those of both previous studies in terms of the CI and the performance of the Acuros XB algorithm. The phantom conducted by Rana et al. using Extradin A1 chamber clearly showed that the Acuros XB algorithm is more accurate for SBRT as compared to AAA, which is in agreement with our phantom study using Diamond detector when the dose is prescribed to medium.

The Acuros XB algorithm provides accuracy comparable to Monte Carlo simulation, as it attempts to simulate all the physical processes affected by beam particles. The dose calculation process of the Acuros XB is faster than that of Monte Carlo simulations. Therefore, it is less time consuming, although the two methods have comparable accuracy.[15,21,31]

5. Conclusion

The C-VMAT technique provided better CIs and HIs as compared to the NC-IMRT and NC-3DCRT treatment techniques. Moreover, the Acuros XB algorithm showed better CIs and HIs compared to the AAA algorithm. In the present study, the dose delivered to the whole lung were high using the C-VMAT method as compared to the NC-IMRT and NC-3D CRT techniques. This study proves that the results obtained for the three treatment techniques using the Acuros XB algorithm are superior to those obtained using the AAA, especially when treating a heterogeneous medium, such as the lung.

Conflict of interest

None declared.

Financial disclosure

None declared.

REFERENCES

1. Park JI, Ye SJ, Kim HJ, Park JM. Dosimetric effects of immobilization devices on SABR for lung cancer using VMAT technique. *J Appl Clin Med Phys* 2015;**16**:5217.
2. Scorsetti M. Stereotactic body radiation therapy: a useful weapon in anticancer treatment. *J Rep Pract Oncol Radiother* 2015;**20**:ix–x.
3. Martin AA. Stereotactic body radiotherapy: a review. *J Clin Oncol* 2010;**22**:157–72.
4. Videtic G, Stephans K, Reddy C, et al. Intensity-modulated radiotherapy-based stereotactic body radiotherapy for medically inoperable early-stage lung cancer: excellent local control. *J Radiat Oncol Biol Phys* 2010;**77**:344–9.
5. Torre LA, Siegel RL, Jemal A. Lung cancer statistics. *J Adv Exp Med Biol* 2016;**893**:1.
6. Chehade S, Palma DA. Stereotactic radiotherapy for early lung cancer: evidence-based approach and future directions. *J Rep Pract Oncol Radiother* 2015;**20**:403–10.
7. Filippi AR, Franco P, Ricardi U. Is stereotactic ablative radiotherapy an alternative to surgery in operable stage I non-small cell lung cancer? *J Rep Pract Oncol Radiother* 2014;**19**:275–9.
8. Bree Id, Van H, Mariëlle GE, Van V, Lieneke R. High-dose radiotherapy in inoperable nonsmall cell lung cancer: comparison of volumetric modulated arc therapy, dynamic IMRT and 3D conformal radiotherapy. *J Med Dosim* 2012;**37**:353–7.
9. Marín A, Martín M, Liñán O, et al. Bystander effects and radiotherapy. *J Rep Pract Oncol Radiother* 2015;**20**:12–21.
10. Amendola BE, Amendola MA, Perez N, Wu X, Suarez JB. Local failure after primary radiotherapy in lung cancer: is there a role for SBRT? *J Rep Pract Oncol Radiother* 2015;**20**:440–5.
11. Weyh A, Konski A, Nalichowski A, Maier J, Lack D. Dosimetric effects of immobilization devices on SABR for lung cancer using VMAT technique. *J Appl Clin Med Phys* 2013;**14**:5217.
12. Lee TF, Chao PJ, Ting HM, et al. Comparative analysis of SmartArc-based dual arc volumetric-modulated arc radiotherapy (VMAT) versus intensity-modulated radiotherapy (IMRT) for nasopharyngeal carcinoma. *J Appl Clin Med Phys* 2011;**12**:3587.
13. Chow JCL, Seguin M, Alexander A. Dosimetric effect of collimating jaws for small multileaf collimated fields. *Med Phys* 2005;**32**:759–65.
14. Knöös T, Wieslander E, Cozzi L, et al. Comparison of dose calculation algorithms for treatment planning in external photon beam therapy for clinical situations. *Phys Med Biol* 2006;**51**:5785.
15. Rana S, Rogers K, Lee T, Reed D, Biggs C. Verification and dosimetric impact of Acuros XB algorithm for stereotactic body radiation therapy (SBRT) and RapidArc planning for non-small-cell lung cancer (NSCLC) patients. *IJMPCERO* 2013;**2**:6.
16. Van EA, Tillikainen L, Pyykkonen J, et al. Testing of the analytical anisotropic algorithm for photon dose calculation. *Med Phys* 2006;**33**:4130–48.
17. Bragg CM, Wingate K, Conway J. Clinical implications of the anisotropic analytical algorithm for IMRT treatment planning and verification. *Radiother Oncol* 2008;**86**:276–84.
18. Rana SB. Dose prediction accuracy of anisotropic analytical algorithm and pencil beam convolution algorithm beyond high density heterogeneity interface. *South Asian J Cancer* 2013;**2**:26.
19. Dunn L, Lehmann J, Lye J, et al. National dosimetric audit network finds discrepancies in AAA lung inhomogeneity corrections. *Phys Med* 2015;**31**:435.
20. Vassiliev ON, Wareing TA, McGhee J, Failla G, Salehpour MR, Mourtada F. Validation of a new grid-based Boltzmann equation solver for dose calculation in radiotherapy with photon beams. *Phys Med Biol* 2010;**55**:581.
21. Bush K, Gagne IM, Zavgorodni S, Ansbacher W, Beckham W. Dosimetric validation of Acuros® XB with Monte Carlo methods for photon dose calculations. *J Med Phys* 2011;**38**:2208–21.
22. Kan MWK, Leung LHT, Peter KN. Verification and dosimetric impact of Acuros XB algorithm on intensity modulated stereotactic radiotherapy for locally persistent nasopharyngeal carcinoma. *Med Phys* 2012;**39**:4705–14.
23. Failla GA, Wareing T, Archambault Y, Thompson S. *Acuros XB advanced dose calculation for the Eclipse treatment planning system*. Palo Alto, CA: Varian Medical Systems; 2010.
24. Prabhakar R, Rath G. Slice-based plan evaluation methods for three dimensional conformai radiotherapy treatment planning. *Australas Phys Eng Sci Med* 2009;**32**:233–9.
25. Benedict SH, Yenice KM, Followill D, et al. Stereotactic body radiation therapy: the report of AAPM Task Group 101. *Med Phys* 2010;**37**:4078–101.
26. http://www.medicalexpo.com/prod/cirs/product-95901-721801.html.
27. Rana S. Clinical dosimetric impact of Acuros XB and analytical anisotropic algorithm (AAA) on real lung cancer treatment plans: review. *Int J Cancer Ther Oncol* 2014;**2**:02019.

28. Holt A, Van VV, Corine M, Anton B, José SD, Eugène MF. Volumetric-modulated arc therapy for stereotactic body radiotherapy of lung tumors: a comparison with intensity-modulated radiotherapy techniques. *Int J Radiat Oncol Biol Phys* 2011;**81**:1560–7.
29. Cai J, Malhotra HK, Orton CG. A 3D-conformal technique is better than IMRT or VMAT for lung SBRT. *Med Phys* 2014;**41**:040601.
30. Liu HW, Nugent Z, Clayton R, Dunscombe P, Lau H, Khan R. Clinical impact of using the deterministic patient dose calculation algorithm Acuros XB for lung stereotactic body radiation therapy. *Acta Oncol* 2014;**53**:324–9.
31. Rana S, Rogers K. Dosimetric evaluation of Acuros XB dose calculation algorithm with measurements in predicting doses beyond different air gap thickness for smaller and larger field sizes. *J Med Phys* 2013;**38**:9–14.